# Carrier Generation and Recombination in *P-N* Junctions and *P-N* Junction Characteristics*

CHIH-TANG SAH†, MEMBER, IRE, ROBERT N. NOYCE†, MEMBER, IRE AND WILLIAM SHOCKLEY†, FELLOW, IRE

*Summary*—**For certain *p-n* junctions, it has been observed that the measured current-voltage characteristics deviate from the ideal case of the diffusion model. It is the purpose of this paper to show that the current due to generation and recombination of carriers from generation-recombination centers in the space charge region of a *p-n* junction accounts for the observed characteristics. This phenomenon dominates in semiconductors with large energy gap, low lifetimes, and low resistivity. This model not only accounts for the nonsaturable reverse current, but also predicts an apparent exp ($qV/nkT$) dependence of the forward current in a *p-n* junction. The relative importance of the diffusion current outside the space charge layer and the recombination current inside the space charge layer also explains the increase of the emitter efficiency of silicon transistors with emitter current. A correlation of the theory with experiment indicates that the energy level of the centers is a few $kT$ from the intrinsic Fermi level.**

## I. Introduction

THE VOLTAGE current characteristics of *p-n* junctions have been studied by many authors. The ideal theory of a *p-n* junction of Shockley accounts for the electrical characteristics of a germanium *p-n* junction quite well at room temperatures.[1] However, it is generally observed that at room temperatures the measured electrical characteristics of silicon *p-n* junctions deviate considerably from that predicated by the ideal theory. For example, Shockley's ideal theory predicts a saturation current for the *p-n* junction under large reverse bias and a simple dependence of the forward current on the applied bias through the Boltzmann's factor of the full applied voltage when the forward bias is several $kT/q$. Usually, at room temperature the current in a silicon *p-n* junction does not saturate at large reverse bias and increases much slower than the Boltzmann's factor to the full applied voltage under forward bias. Discrepancy has also been observed by many workers between the ideal theory for *p-n* junction transistors and the observed characteristics of silicon *p-n* junction transistors. In particular, the ideal theory predicts a nearly unity value for the transistor current amplification factor, alpha, at low emitter current densities, while the observed alpha usually becomes very small at low emitter current densities.[2,3]

It has been pointed out by Shockley and Read[4] that generation of the current carriers in the space charge region or the transition layer of a *p-n* junction may be extremely high. The essential features of the reverse characteristics of a silicon *p-n* junction can be understood in terms of this phenomenon by using a model of single energy level uniformly distributed Shockley-Read-Hall recombination centers. Pell and Roe,[5] and Kleinknecht and Seiler[6] have independently used this model to account for the reverse characteristics of silicon *p-n* junctions.

Shockley has suggested that the recombination of the carriers may also dominate in the space charge region when a *p-n* junction is biased in the forward direction.[1] However, the importance of this effect on the *p-n* junction and junction transistor characteristics has not been realized until recently.[7]

In this paper, we present a physical theory of *p-n* junctions taking into account the recombination and generation of the carriers in the space charge region or the transition region.

## II. Shockley-Read-Hall Recombination Statistics

A brief derivation is given in this section for the steady-state recombination statistics of electrons and holes in semiconductors to illustrate the method and physical principle involved. For a complete and detailed treatment of this subject, the reader is referred to Shockley and Read.[4]

The recombination and generation of electrons and holes in semiconductors may take place at some type of recombination-generation centers or traps. These sites may be crystal lattice dislocations, impurity atoms located interstitially or substitutionally in the crystal lattice, or surface defects. Recombination may also oc-

* Original manuscript received by the IRE, March 23, 1957; revised manuscript received, May 13, 1957.

† Shockley Semiconductor Lab., Mountain View, Calif.

[1] W. Shockley, "The theory of *p-n* junctions in semiconductors and *p-n* junction transistors," *Bell Sys. Tech. J.*, vol. 28, pp. 435–489; July, 1949.

[2] J. L. Moll, *et al.*, "*P-N-P-N* transistor switches," PROC. IRE, vol. 44, pp. 1174–1182; September, 1956.

[3] M. Tanenbaum and D. E. Thomas, "Diffused emitter and base silicon transistors," *Bell Sys. Tech. J.*, vol. 35, pp. 1–22; January, 1956.

[4] W. Shockley and W. T. Read, Jr., "Statistics of recombinations of holes and electrons," *Phys. Rev.*, vol. 87, pp. 835–842; September, 1952.
R. N. Hall, "Germanium rectifier characteristics," *Phys. Rev.*, vol. 83, p. 228; July, 1951.
R. N. Hall, "Electron-hole recombination in germanium," *Phys. Rev.*, vol. 87, p. 387; July, 1952.

[5] E. M. Pell and G. M. Roe, "Reverse current and carrier lifetime as a function of temperature in germanium junction diodes," *J. Appl. Phys.*, vol. 26, pp. 658–665; June, 1955.

[6] H. Kleinknecht and K. Seiler, "Einkristalle und *pn* Schichtkristalle aus Silizium," *Z. Physik*, vol. 139, pp. 599–618; December 20, 1954.

[7] R. N. Noyce, C. T. Sah, and W. Shockley, "Carrier generation and recombination in the space charge region of a *p-n* junction," *Bull. Amer. Phys. Soc. II*, vol. 1, H9, p. 382; December 27, 1956.
C. T. Sah, and W. Shockley, "Interpretation of silicon *p-n* junction current-voltage characteristics," *Bull. Amer. Phys. Soc. II*, vol. 1, H10, p. 382; December 27, 1956.

cur directly with the emission of light or by the three (or more) particle process (Auger process) with the third carrier carrying away the energy. The radiative process is rather improbable. At present, there is no sufficient information about the Auger process in semiconductors. Thus, these processes will not be considered.

Under steady-state conditions, a single energy level recombination center is characterized by three numbers: the capture cross section for electrons, the capture cross section for holes, and the energy involved in these transitions. The cross sections are inversely proportional to the lifetimes of electrons and holes respectively, and the transition energy may be measured from one of the edges of the energy gap of the semiconductor.[8]

There are four basic processes involved in the carrier generation and recombination through the traps.[4] If a trap is occupied by a hole, an electron may drop into the trap from the conduction band and recombine with the hole, or the trap may emit the hole to the valence band. If the trap is initially filled with an electron, the trapped electron may be emitted to the conduction band or a valence band hole may move into the trap and recombine with the trapped electron. These four processes are illustrated in Fig. 1. The direction of the arrow indicates

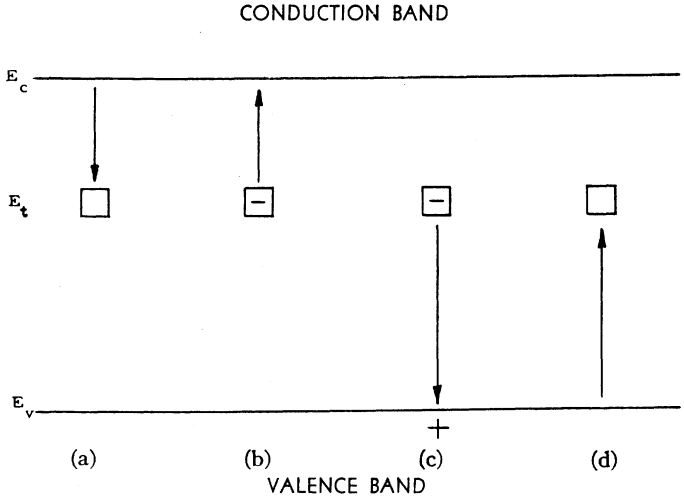


Fig. 1—The basic processes of carrier generation and recombination through traps, (a) electron capture, (b) electron emission, (c) hole capture, (d) hole emission.

the direction of transition for either a conduction or a valence band electron as the case may be.

Consider the electron capture process indicated by Fig. 1(a). The rate that the electron in the conduction band will drop into an empty trap is

$$nf_{tp}/\tau_{n0}. \tag{1}$$

(See Table I for the meaning of the symbols.)

The electron emission rate indicated by Fig. 1(b) can be written as

$$af_t, \tag{2}$$

[8] The steady-state recombination statistics involving centers with more than one energy level has also been considered by the authors. (To be published.)

TABLE I

SYMBOLS

$n$ = density of electrons in the conduction band $= n_i \exp (F_n - E_i)/kT$
$p$ = density of holes in the valence band $= n_i \exp (E_i - F_p)/kT$
$E_v$ = energy of the highest valence band level
$E_c$ = energy of the lowest conduction band level
$E_i$ = intrinsic Fermi level $= -q\Psi$
$E_t$ = energy level of the recombination-generation centers or traps
$\epsilon_t = (E_t - E_i)/kT + \ln \sqrt{\tau_{p0}/\tau_{n0}}$
$\Psi$ = electrostatic potential $= -E_i/q$
$\Psi_D$ = diffusion or built-in voltage in a $p$-$n$ junction
$\phi_n$ = quasi-Fermi electrostatic potential or imref for electrons $= -F_n/q$
$\phi_p$ = quasi-Fermi electrostatic potential or imref for holes $= -F_p/q$
$n_i$ = density of electrons or holes in an intrinsic specimen
$N_c$ = effective density of levels for conduction band
$N_v$ = effective density of levels for valence band
$N_t$ = density of the recombination-generation centers or traps
$f_{tp}$ = fraction of traps occupied by holes
$f_t$ = fraction of traps occupied by electrons $= 1 - f_{tp}$
$n_1$ = density of electrons in the conduction band when the Fermi level falls at $E_t = n_i \exp (E_t - E_i)/kT$
$p_1$ = density of holes in the valence band when the Fermi level falls at $E_t = n_i \exp (E_i - E_t)/kT$
$\tau_{n0}$ = lifetime for electrons injected into highly $p$-type specimen
$\tau_{p0}$ = lifetime for holes injected into highly $n$-type specimen
$q$ = magnitude of electronic charge
$k$ = Boltzmann constant
$T$ = absolute temperature
$U_{cn}$ = net electron capture rate
$U_{cp}$ = net hole capture rate
$U$ = steady-state electron or hole recombination rate
$J_{rg}$ = recombination-generation current density in the space charge layer
$J_D$ = diffusion current density outside the space charge layer

where $a$ is a proportionality factor which includes the trap density, the total number of empty electronic states in the conduction band and the probability of electron emission from the traps. The expression for $a$ can be obtained by a detailed balance argument for the system under the thermal equilibrium condition. Under this condition, the electron emission rate must be equal to the electron capture rate, *i.e.*, (1) and (2) are equal. Thus, if the occupancy of the traps is expressed in terms of a quasi-Fermi level[4] (or imref) for traps $F_t$, then the imref for electrons, $F_n$, must fall at $F_t$ at thermal equilibrium. Assuming that the semiconductor is nondegenerate, and using[9]

$$f_t = (1 + \exp (E_t - F_t)/kT)^{-1}$$

then from equating (1) and (2) we obtain

$$a = n_1/\tau_{n0}. \tag{3}$$

The net capture rate for electrons by the traps under nonequilibrium conditions can then be written as

$$U_{cn} = (nf_{tp} - n_1 f_t)/\tau_{n0}. \tag{4}$$

An entirely similar treatment can be carried out for holes leading to the following equation for the net rate of capture for holes under nonequilibrium conditions.

$$U_{cp} = (pf_t - p_1 f_{tp})/\tau_{p0}. \tag{5}$$

[9] Electron spin degeneracy is included in $E_t$.

The rate of recombination for nonequilibrium but steady-state conditions is obtained by requiring that the net rate of capture of electrons be equal to that of holes. This condition leads to

$$U = U_{cn} = U_{cp}$$
$$= (pn - n_i^2)/[(n + n_1)\tau_{p0} + (p + p_1)\tau_{n0}] \quad (6)$$

for the steady-state recombination rate for electrons or holes.

The result of these statistics is applied to the current carriers in the transition region of a $p$-$n$ junction and in the region outside of the transition region.

## III. Idealized Model

An idealized $p$-$n$ junction is considered in this section so that the physical processes can be readily visualized. It is assumed that there are single-level, uniformly-distributed recombination-generation centers located at the intrinsic Fermi level. Thus $p_1 = n_1 = n_i$. It is further assumed that the lifetimes, mobilities, and the densities of the minority carriers on opposite sides of the junction are equal. The recombination and generation processes are considered separately in the $p$ region, the $n$ region, and the transition region of a $p$-$n$ junction.

In the $p$ region shown in Fig. 2(a), the traps are mostly empty and ready to trap the injected electrons. Subsequently, the holes would move into these occupied traps and recombine with the trapped electrons. In order to preserve electrical neutrality, holes must be replenished through electron current flowing in the external circuit. Thus, with $p = p_p \gg p_1$, $n_1$ and $n$, and $n = n_p + \Delta n$, (6) reduces to

$$U = (n - n_p)/\tau_{n0}. \quad (7)$$

Similarly, the recombination rate in the $n$ region, shown in Fig. 2(b), is given by

$$U = (p - p_n)/\tau_{p0}. \quad (8)$$

These are the usual linear recombination laws which hold when the injected minority carrier density is much smaller than the equilibrium carrier density.

If the minority carriers are rapidly moving out of a certain region of the semiconductor by electric field, the generation rates in this region would be

$$-U = n_p/\tau_{n0}, \quad (7a)$$

for $p$-type region, or

$$-U = p_n/\tau_{p0} \quad (8a)$$

for $n$-type region. The edges of the space charge layer of a reversely biased $p$-$n$ junction are precisely the regions where (7a) and (8a) prevail. On the average, a minority carrier generated in the $n$ region or the $p$ region within one diffusion length from the edge of the space charge layer would diffuse to the edge and slide down the potential hill of the space charge region rapidly.[1] Thus,

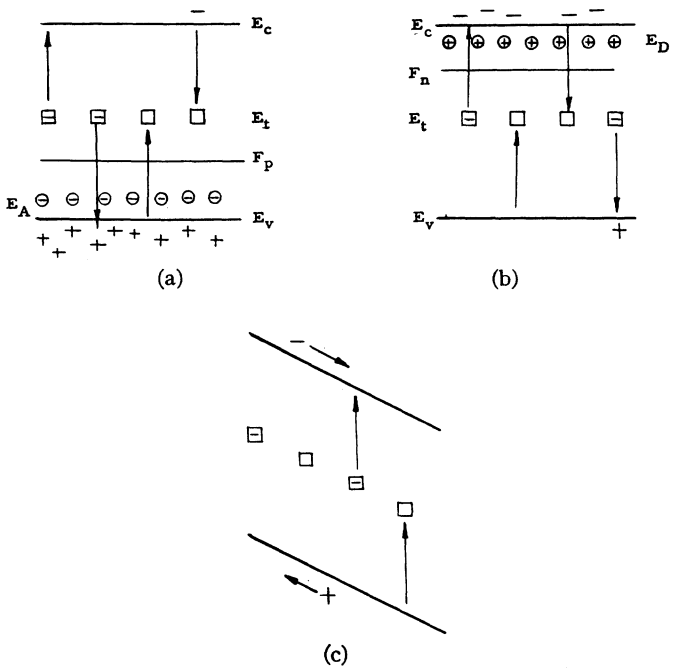


Fig. 2—Recombination and generation processes in semiconductor, (a) $p$ region, (b) $n$ region, (c) intrinsic with swept field.

the current which must flow in the external circuit to replenish the diffusing minority carriers is

$$J_d A = -2qn_p L_0 A/\tau_0, \quad (9)$$

where $n_p = p_n$ and $\tau_{n0} = \tau_{p0} = \tau_0$ have been used. $L_0$, the diffusion length of the minority carrier, is given by $(D_0\tau_0)^{1/2}$, and $D_0 = D_n = D_p$ is the diffusion constant of the minority carriers. $A$ is the area of the junction.

Let us next consider the space charge region or the transition region of a reversely biased $p$-$n$ junction. Both types of carriers are rapidly swept out of this region by the large electric field, thus their densities are small compared to $n_i$. The situation is shown in Fig. 2(c). For this case, the generation rate from (6) is

$$-U = n_i/2\tau_0, \quad (10)$$

and is approximately constant over the entire space charge layer. It may be noted that the recombination effect is again unimportant here because of the presence of the large electric field. It may also be noted that the centers are about half empty and half filled in this region.

Since for every pair of carriers generated, one electron must flow in the external circuit, the current flowing in the external circuit due to this effect is

$$J_{rg}A = -qWn_iA/2\tau_0, \quad (11)$$

where $W$ is the width of the space charge layer.

The currents generated in the $p$ region and the $n$ region and the current generated in the space charge layer may be compared. The ratio of these two components given by (9) and (11) is

$$J_{rg}/J_d = (n_n/4n_i)W/L_0. \quad (12)$$

A number of conclusions regarding the relative importance of these two currents can be deduced. Eq. (12) indicates that the current generated in the space charge region may be extremely large compared with the diffusion current for semiconductors with short lifetimes, low resistivities, large energy gap and at low temperatures, even if $W \ll L_0$.

For a typical example, consider a 2 ohm-cm material of one microsecond lifetime. Assuming a one micron space charge layer width, at room temperature the current ratio is about 3000 for a silicon $p$-$n$ junction while it is only about 0.1 for a germanium $p$-$n$ junction. Thus, the generation-recombination current in the space charge layer would greatly influence the characteristics of silicon semiconductor devices.

If the current due to generation in the space charge layer is important under the reverse bias condition, it would be expected that the reverse process, namely, recombination in the space charge layer, will be important under forward bias. However, the extension of the argument for deriving the current produced in the space charge layer must take a slightly different form from that applied to the reverse-bias case.

Under forward bias, the carrier concentrations at the center of the space charge region are equal and vary as

$$n = p = n_i \exp (qV/2kT), \tag{13}$$

since $np = n_i^2 \exp (qV/kT)$. The recombination rate at this $p$-$n$ boundary is then

$$U = n_i \exp (qV/2kT)/2\tau_0 \tag{14}$$

for $V$ greater than several $kT/q$, and falls exponentially with distance on either side of the $p$-$n$ boundary with a characteristic length of $kT/qE$ where $E$ is the electric field at the junction. Thus, the recombination current density is

$$J_{rg} = 2(kT/qE)qn_i \exp (qV/2kT)/2\tau_0, \tag{15}$$

where the factor 2 comes from the contribution on the two sides of the $p$-$n$ boundary. The exact expression for this idealized case involves an additional factor of $\pi/2$, which takes into account that the recombination rate falls slower than $\exp (-qEx/kT)$ near $x = 0$.

The sum of the diffusion current densities which flow in the $p$ region and the $n$ region is given by[1]

$$J_D = (2qn_pL_0/\tau_0) \exp (qV/kT) \tag{17}$$

for applied forward bias of several $kT/q$. The two currents can again be compared, giving a current ratio of

$$J_{rg}/J_D = (n_i/n_p)(W/2L_0)[kT/q(\Psi_D - V)] \cdot \exp (-qV/2kT). \tag{18}$$

Using the same data as in (12) with a space charge layer width of 0.1 micron, the recombination current becomes equal and greater than the diffusion current at applied bias of less than 10 $kT/q$.

The total current per unit area is given by the sum of the diffusion and the recombination-generation current densities. The comparison given above indicates that the recombination-generation current is much greater than the diffusion current, and the total current would vary slower than the ideal rectifier formula of $\exp (qV/kT)$.

## IV. Theoretical Calculation of the Current-Voltage Characteristics

In the last section and in the literature,[1,4] an effective lifetime, which is a function of the carrier densities, has been used to obtain the characteristics of $p$-$n$ junction devices. The effective lifetime is usually obtained by experimental measurements. In order to obtain a complete theoretical relation between the current and the applied voltage, it is necessary to start with the exact expression of the steady-state recombination rate of the carriers given by (6).

Substitution of the following relations

$$\begin{aligned} p_1 &= n_i \exp (E_i - E_t)/kT \\ n_1 &= n_i \exp (E_t - E_i)/kT \\ p &= n_i \exp (\phi_p - \Psi)q/kT \\ n &= n_i \exp (\Psi - \phi_n)q/kT \\ E_i &= (E_c + E_v - kT \ln N_c/N_v)/2 = -q\Psi \end{aligned} \tag{19}$$

into (6) gives the following expression for the steady-state recombination rate:

$$U = \frac{n_i}{\sqrt{\tau_{p0}\tau_{n0}}} \cdot \frac{\sinh \frac{q}{2kT}(\phi_p - \phi_n)}{\cosh \left[\frac{q}{kT}\left(\Psi - \frac{\phi_p + \phi_n}{2}\right) + \ln \sqrt{\frac{\tau_{p0}}{\tau_{n0}}}\right] + \exp \left[\frac{-q}{2kT}(\phi_p - \phi_n)\right] \cosh \left(\frac{E_t - E_i}{kT} + \ln \sqrt{\frac{\tau_{p0}}{\tau_{n0}}}\right)} \tag{20}$$

Using a linear potential variation across the junction, the electric field can be written as

$$E = (\Psi_D - V)/W \tag{16}$$

where $\Psi_D$ is the built-in voltage.

The notations are identical to those used by Shockley and Read,[4] and are listed in Table I.

The recombination rate given above is sketched for several limiting conditions in Fig. 3.

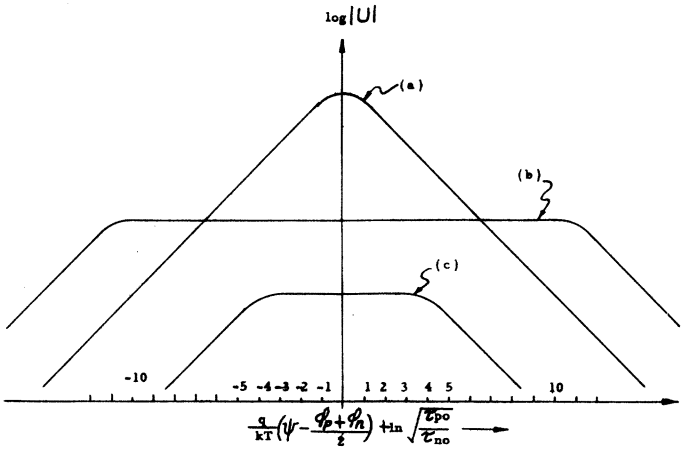


Fig. 3—Variation of the recombination rate in the $p$-$n$ junction transition region; (a) forward bias $(\phi_p-\phi_n)q/2kT\gg 1$, $|(E_t-E_i)/kT+\frac{1}{2}\ln \tau_{p0}/\tau_{n0}|$, (b) reverse bias $(\phi_n-\phi_p)q/2kT\gg 1$, $|(E_t-E_i)/kT+\frac{1}{2}\ln \tau_{p0}/\tau_{n0}|$, (c) small bias $(\phi_p-\phi_n)q/2kT\doteq 1$, $|(E_t-E_i)/kT\frac{1}{2}\ln \tau_{p0}/\tau_{n0}|\doteq 4$.

The recombination-generation current in the space charge layer is obtained by integrating (20) over the space charge layer. For the one-dimensional case, the total recombination-generation current density in the space charge layer is given by

$$J_{rg} = q\int U dx, \tag{21}$$

where the integration is taken over the space charge layer.

The exact solution of this problem requires a knowledge of the imrefs $\phi_p$ and $\phi_n$ and the electrostatic potential $\Psi$ as a function of position in the $p$-$n$ junction. This is a difficult problem involving the solution of simultaneous nonlinear differential equations.[1] In this treatment, we shall follow a self-consistent approach given in Appendix I. It is convenient to consider three regions of the applied bias, the large reverse-bias region, the small bias region, and the large forward-bias region.

*Large Reverse-Bias, $-q(\phi_p-\phi_n)/kT\gg 1$*

For this case, the potential energy diagram for holes is shown in Fig. 4 together with the current distribution in the $p$-$n$ junction. The hole current $J_p$ shown in the lower part of Fig. 4 can be deduced from the recombination-generation rate and (21). Under large reverse-bias, the first term in the denominator of (20) is small compared with the second term, since $\phi_n-\phi_p$ is several $kT/q$ inside the space charge layer. Thus, the recombination rate is approximately constant over the entire transition region as illustrated in Fig. 3(b). The hole current then is proportional to the distance and decreases monotonically. The total recombination-generation current for this case is then

$$J_{rg} = qUW, \tag{22}$$

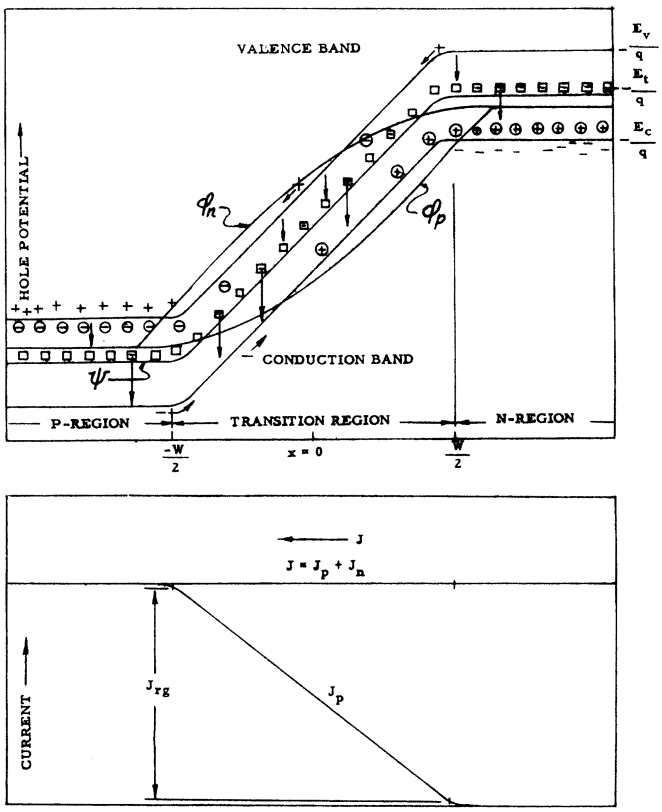


Fig. 4—$p$-$n$ junction under large reverse bias.

where $W$ is the space charge layer width and the generation rate is given by

$$-U = n_i\left[2\sqrt{\tau_{p0}\tau_{n0}}\cosh\left(\frac{E_t-E_i}{kT}+\frac{1}{2}\ln\frac{\tau_{p0}}{\tau_{n0}}\right)\right]^{-1}. \tag{23}$$

This approximation slightly overestimates the generation current since the generation rate drops exponentially to zero near the edges of the space charge layer.

The result obtained above indicates that the traps are most effective as generation centers if they are located at the intrinsic Fermi level when the lifetimes of the carriers are equal. In general, the traps are most effective if $(E_t-E_i)/kT+(1/2)\ln \tau_{p0}/\tau_{n0}=0$. The above result also shows that the generation current cannot saturate. For the linear-graded junction this current is proportional to $\frac{1}{3}$ power of the applied voltage and for a step junction it is proportional to $\frac{1}{2}$ power of the applied voltage since the space charge layer width varies accordingly.

Although it was shown that the shapes of the imrefs have negligible effect on the calculation of the generation-recombination rate, it is instructive to deduce the shapes of the imrefs. From the relation between the hole current and the imref for holes,

$$J_p = -qn_i\mu_p \exp\left[(\phi_p-\Psi)q/kT\right]d\phi_p/dx, \tag{24}$$

it can be concluded that in the transition region, the increase of the slope of $\phi_p$ must be slower than the decrease

of the hole density $p$ or the factor $\exp(\phi_p - \Psi)q/kT$ in order to give a monotonic variation of $J_p$. A similar consideration can be given to the electron imref variation in the transition region. These arguments lead to the potential diagram shown in Fig. 4. The drop of the imrefs is almost complete inside the space charge layer. A numerical calculation in Appendix I for a silicon junction also gives the same conclusion.

It is interesting to note that the product of the junction capacity and the space charge layer generated current is a constant under large reverse-bias and is independent of the shape of the electrostatic potential distribution inside the junction. This relation can be written as

$$CJ_{rg} = \epsilon_0 KqU, \tag{25}$$

where $\epsilon_0$ is the permittivity of free space and $K$ is the dielectric constant. The constancy of the product given above holds only at intermediate range of applied voltage. At reverse-bias near the avalanche breakdown, the product given by (25) increases. The lifetimes $\tau_{n0}$ and $\tau_{p0}$ may be field dependent and cause additional variation of the product with the reverse-bias.

The avalanche mechanism is considered in detail in Appendix II. The effect of the avalanche multiplication is to multiply the recombination-generation current in the same way as if it were injected into the space charge layer if the electron and hole ionization rates are equal. Thus, for large reverse-bias, the recombination-generation current is given by

$$J_{rg} = qUWM, \tag{22a}$$

where $M$ is the avalanche multiplication factor given in Appendix II.

The thermal activation energy or the energy level of the recombination-generation centers can be obtained readily by temperature measurement of the reverse characteristics. The magnitude of the trap energy level from the intrinsic Fermi level is given by the difference of half the zero temperature energy gap width and the activation energy obtained from the slope of a plot of $\ln J_{rg} - (5/2)\ln kT$ vs $(kT)^{-1}$. The detailed calculation is given in Appendix III.

*Small Applied Bias*

For this case, both terms in the denominator of the expression for $U$ are important and one has to consider the shape of the imrefs in order to obtain a good approximation to $\Psi - (\phi_p + \phi_n)/2$ in the expression for $U$. A similar argument for the shape of the imrefs as that given to the large reverse-bias case can be made here. This leads to the conclusion that the variation of the imrefs in the space charge layer is very small, contrary to the result of the large reverse-bias case. This is also confirmed by a numerical calculation given in Appendix I. Outside the space charge region the imrefs vary linearly with distance. The approximate potential energy diagram and the current distribution across the junction is shown in Fig. 5 from these conclusions. The current shown there is for a case where the recombination current is about 2.5 times higher than the total diffusion outside the space charge layer.

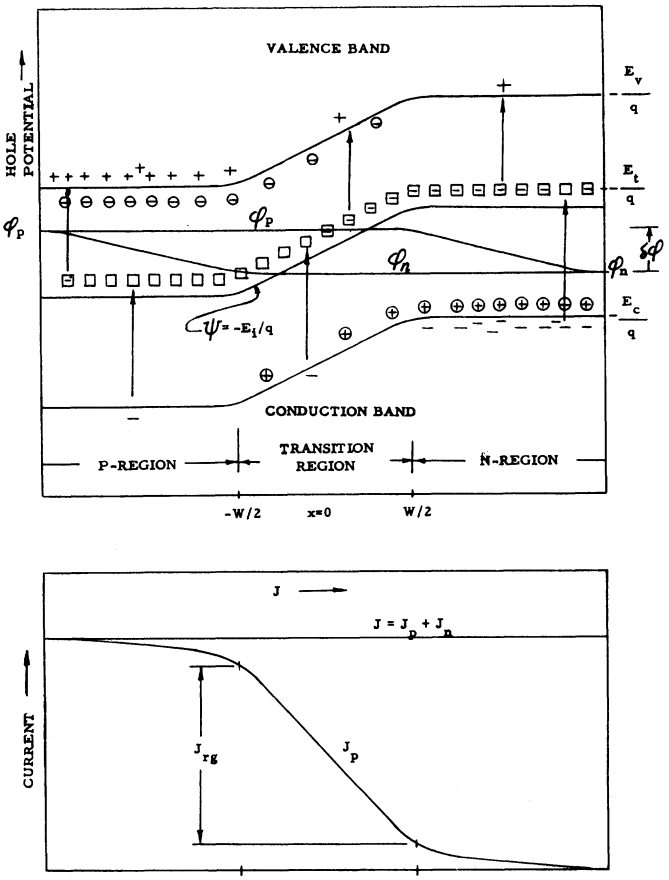


Fig. 5—$p$-$n$ junction under forward bias.

From Fig. 5, it can be seen that the electrostatic potential can be written approximately

$$\Psi - \frac{\phi_p + \phi_n}{2} = \frac{\Psi_D - (\phi_p - \phi_n)}{W}\, x \quad -\frac{W}{2} < x < \frac{W}{2}, \tag{26}$$

where $W$ is the total space charge layer width, $\phi_p - \phi_n$ is approximately the applied voltage and $\Psi_D$ is the built-in voltage or the difference of the intrinsic Fermi levels on the two sides of the junction. An exact expression for the electrostatic potential variation could be obtained.[1] However, a linear approximation given by (26) will give a maximum of 50 per cent error in the slope of $\Psi$ and will put the integral of (21) into a more tractable form.[10]

[10] Dr. Ruth F. Schwarz of Philco Corporation has kindly sent us her more exact calculation for step junctions. The linear approximation of (26) is quite good for grown or diffused type graded-junctions.

Performing the integration, the recombination current can be written as

$$J_{rg} = \frac{qn_i}{\sqrt{\tau_{p0}\tau_{n0}}} W \frac{2 \sinh (\phi_p - \phi_n)q/2kT}{(\Psi_D - \phi_p + \phi_n)q/kT} f(b), \quad (27)$$

where

$$f(b) = \int_{z_1}^{z_2} \frac{dz}{z^2 + 2bz + 1}$$

$$b = \exp [-(\phi_p - \phi_n)q/2kT] \cdot \cosh \left[\frac{E_t - E_i}{kT} + (1/2) \ln (\tau_{p0}/\tau_{n0})\right]$$

and the integration limits are

$$z_{1,2} = (\tau_{p0}/\tau_{n0})^{1/2} \exp [\mp(\Psi_D - \phi_p + \phi_n)q/2kT].$$

The integral given by $f(b)$ can be evaluated exactly. However, at applied voltages several $kT/q$ less than the built-in voltage, the integration limits can be extended from zero to infinity with small error. The value of the integral and its slope is plotted in Fig. 6 for the case of $z_1 = 0$ and $z_2 = \infty$. The variation of the slope of log $J_{rg}$ is also plotted in Fig. 7.

There are several regions of the current-voltage characteristics for this case which need special discussion.

1) *Very Small Bias:* When the applied bias is less than $kT/q$, the recombination-generation current follows essentially the ohmic law. The recombination conductance at zero bias is given by

$$R_{rg}^{-1} = qn_i W f(b)/\sqrt{\tau_{p0}\tau_{n0}}\Psi_D. \quad (28)$$

A comparison of this resistance with the diffusion resistance gives the same conclusions for the relative importance of the two currents as that obtained in Section II.

2) *Medium Forward-Bias with Deep Traps:* When the traps are located near the intrinsic Fermi level, the function $f(b)$ increases slightly when the forward-bias decreases. Thus the recombination current will vary slightly faster than exp $(qV/2kT)$ as can be seen from (27). This is in agreement with the result obtained in Section II from intuitive arguments.

3) *Small or Medium Forward-Bias with Shallow Traps:* A region of small or medium bias with values of $b$ greater than 10 may exist, if the traps are quite shallow, *i.e.*, the effective trap level is about $10kT$ from the intrinsic Fermi level. The integral given by $f(b)$ will vary approximately as $1/b$ and the recombination current will vary with the applied voltage approximately as exp $(qV/kT) - 1$ shown in Fig. 7.

The result given by (27) would reduce to that given by (22) and (23). However, (27) is not accurate in the transition region between small and large reverse bias because of the error in estimating the shape of the imrefs.

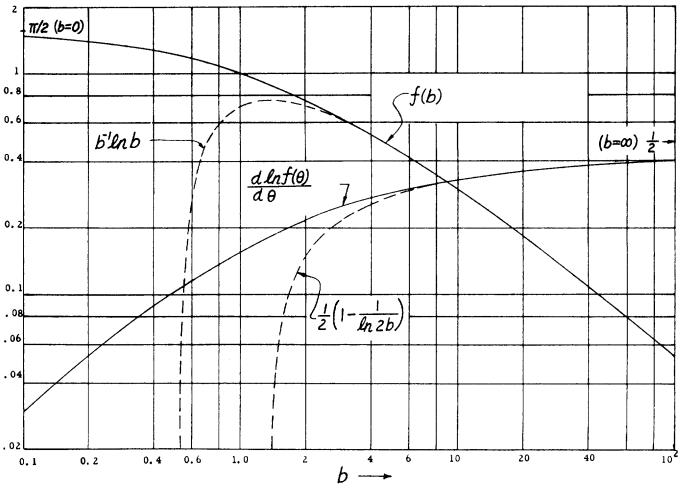


Fig. 6—The function $f(b)$ and its slope.

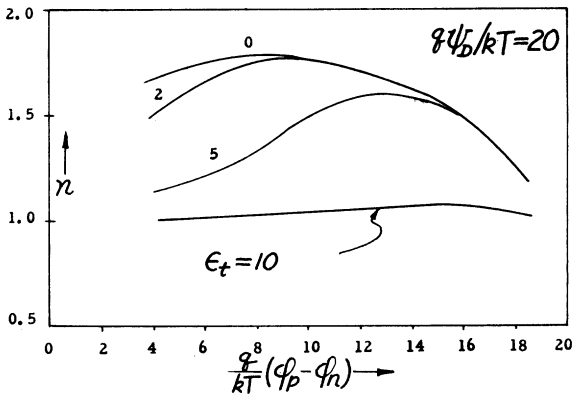


Fig. 7—Slope of ln $J_{rg}$ vs forward applied bias.

*Large Forward-Bias*

At forward-bias about or greater than the built-in voltage, the width of the space charge layer is small. The recombination current in the space charge layer is negligible compared with the diffusion current due to injected carriers outside the space charge layer. We shall consider the case for which the injected carrier density is much higher than the fixed impurity charge concentration in the $n$ region. One may assume for this case that $n \approx p$. The boundary condition at the junction becomes

$$n(0) = p(0) = n_i \exp (qV/2kT), \quad (29)$$

where $V$ is the applied voltage less the ohmic drop. The usual diffusion formula applies and the total current is nearly equal to the hole current at the junction. Thus

$$J = J_p(0) = 2(qD_p n_i/L_0) \exp (qV/2kT), \quad (30)$$

where $L_0$ is an effective diffusion length given in Appendix IV. A more detailed treatment of the diffusion current is given there also. We may note that the region of exp $(qV/2kT)$ occurs at higher applied voltage for the diffusion current than the same case for the recombina-

tion current. The case for the diffusion current has been observed for certain $P^+$ $IN$ diodes with very low ohmic drops.[11]

At still higher current density or applied bias, the current will eventually be limited by the ohmic contact resistance and the bulk resistance of the material. The current voltage characteristics become linear in this range.

To summarize the theoretical calculation, the characteristics of a linearly graded junction is sketched in Fig. 8. Fig. 8(a) shows the reverse characteristics and Fig. 8(b) shows the forward characteristics including the diffusion current outside the space charge layer at large forward bias. For an actual case the regions of distinct but different slopes shown in Fig. 8(b) would merge and a varying slope of between 0.5 and 1 would be observed. From these considerations, we may also conclude here that the minority carrier concentrations at the boundary cannot vary faster than exp $(qV/kT)$. This is in agreement with statistical mechanics considerations.

## V. The Emitter Efficiency and the Current Amplification Factor of a $p$-$n$ Junction Transistor

Carrier recombination in the space charge layer of a forward-biased emitter may play an important role in the determination of the emitter efficiency of a silicon junction transistor at low emitter current. This effect thus imposes a lower limit on the emitter current density for high emitter efficiency operation.

From the theoretical considerations given in the previous sections, the recombination process is dominant in a forward-biased silicon emitter junction. The portion of the emitter current due to this mechanism consists of carrier recombination in the space charge layer and thus is not available for transistor action. At high emitter current, the diffusion current dominates and the emitter efficiency increases. This phenomenon has been observed for silicon transistors.[2,3] The recombination in the space charge layer which causes increasing transistor alpha with current is also the basis for the operation of low current $p$-$n$-$p$-$n$ transistor switches.[2]

The dc transistor current amplification factor, alpha, can be calculated by the following expression at reverse collector bias when the recombination in the emitter space charge layer is taken into consideration.

$$\alpha = \operatorname{sech}(W_b/L_b)\left\{1+\left[(J_{rg}+J_d')/J_d \tanh(W_b/L_b)\right]^{-1}\right. . \quad (31)$$

$J_d$ and $J_d'$ are the injected current densities flowing into the base and the emitter region respectively. $L_b$ is the minority carrier diffusion length in the base and $W_b$ is the base layer width. It is evident from the calculations

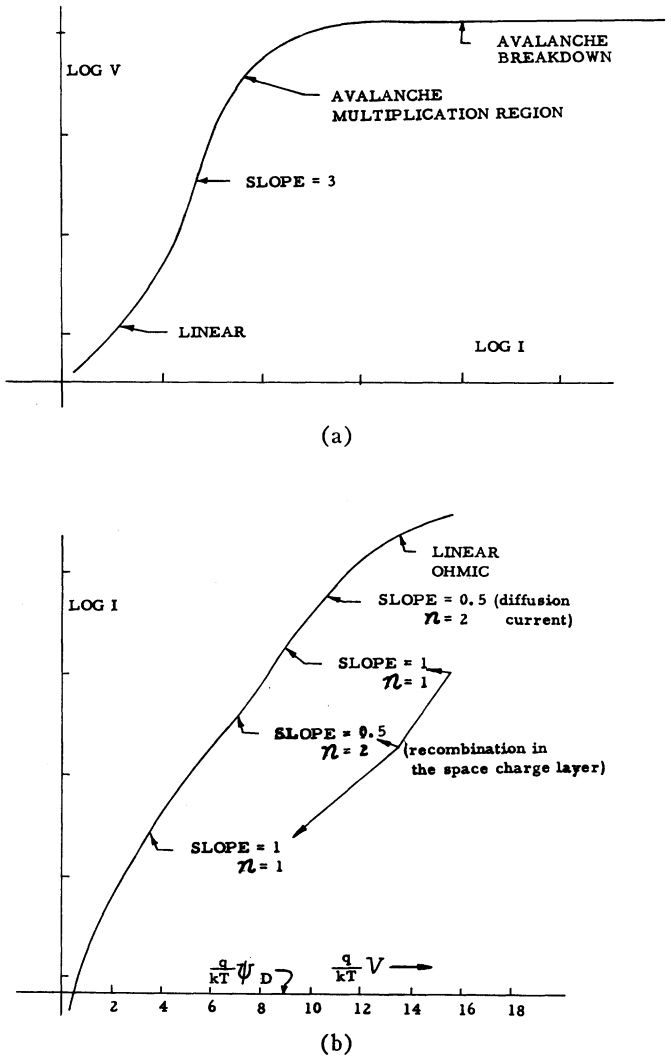


Fig. 8—Characteristics of a linearly graded $p$-$n$ junction, (a) reverse bias, (b) forward bias.

made in the previous section that the dc transistor alpha given by (31) approaches zero at low emitter current density since $J_d \ll J_{rg}$. At large forward bias the alpha increases toward unity since $J_d \gg J_{rg}$, $J_d'$. At still higher emitter current densities, $J_d$, $J_d' \gg J_{rg}$, the emitter efficiency or the alpha decreases as pointed out by Webster.[12]

The proximity of the collector junction increases the diffusion current component and increases the alpha of the device at low emitter current densities.

Fig. 9 shows the current distribution in a $p$-$n$ junction transistor under various emitter bias conditions. Fig. 10 shows several calculated transistor alpha using (31) and the calculated result for the diode shown in the next section. These theoretical curves follow closely the experimental alpha of Moll[2] and Tanenbaum.[13]

[11] R. N. Hall, "Power rectifiers and transistors," Proc. IRE, vol. 40, pp. 1512–1519; November, 1952.

[12] W. M. Webster, "On the variation of junction-transistor current amplification factor with emitter current," Proc. IRE, vol. 42, pp. 914–920; June, 1954.

[13] We are indebted to J. L. Moll for pointing out a numerical error.

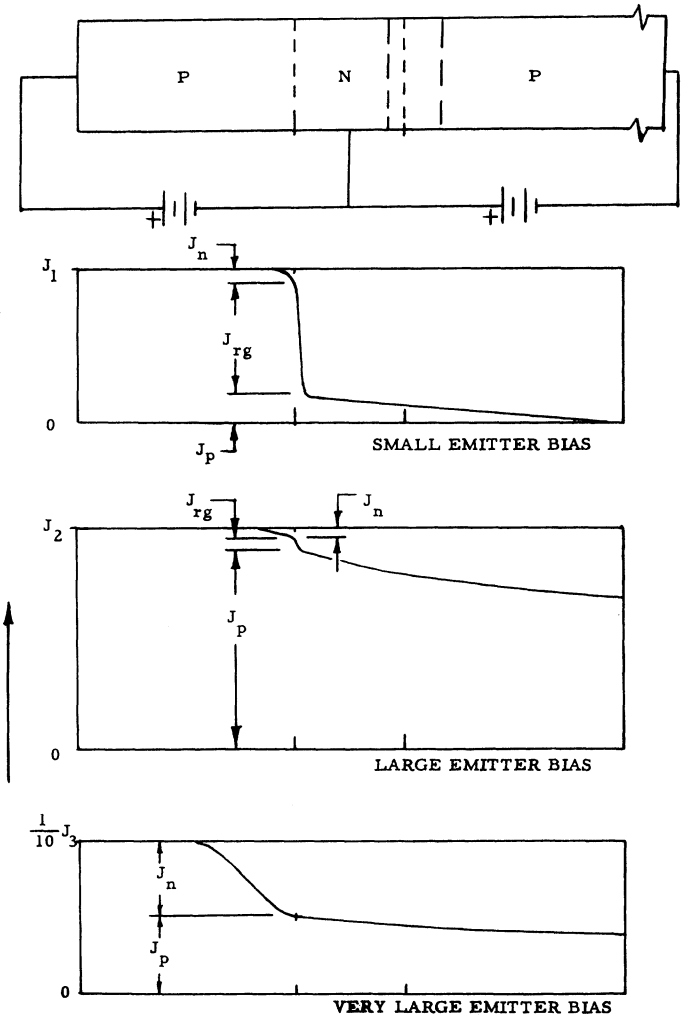


Fig. 9—Current in junction transistor with large carrier recombination in the emitter junction.

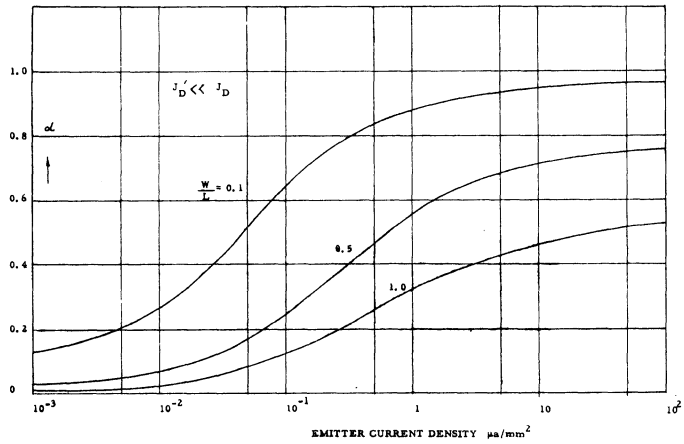


Fig. 10—*p-n-p* silicon transistor dc alpha.

## VI. Experimental Measurements

The experimental *p-n* junctions were produced by diffusion of boron from the gaseous phase into an *n*-type silicon of 2.4 ohm-cm resistivity at 1250°C for 80″.

The following data are obtained from measurements of a typical diffused junction and from calculations.

Bulk concentration $N_D = 2.2 \times 10^{15}$ cm$^{-3}$
Surface concentration of boron $= 4 \times 10^{21}$ cm$^{-3}$
$(D\tau)^{1/2}$ diffusion length of boron $= 1.8$ microns
Junction depth $= 11.8$ microns from surface
Breakdown voltage $= 120$ volts (calculated from results in Appendix II)
Built-in voltage $= 0.47$ volt (see Shockley,[1] with linear graded junction approximation)
Area of junction 0.620 mm$^2$.

In order to calculate the theoretical *p-n* junction characteristics we shall use the linear-graded junction approximation. The trap level $E_t - E_i$ and lifetimes are obtained by matching the theoretical formula and the experimental data at three points. It is most convenient to use two points at relatively small applied bias where the current from the space charge layer is dominant and one point at large forward bias where the diffusion current dominates. We choose these points to be at applied bias of $\theta = qV/kT = -4.6, 4.6$, and $+18.3$. The last point corresponds to the built-in voltage at room temperature. The currents at these voltages are $2.96 \times 10^{-10}$, $3.75 \times 10^{-9}$, and $1.0 \times 10^{-4}$ amperes respectively from Figs. 11 and 12.

Using (27) for the first two points and the formula for diffusion current given in Appendix IV we obtain the following results:

$$\tau_{p0} = 1.2 \times 10^{-8} \text{ sec},$$
$$\tau_{n0} = 4.3 \times 10^{-6} \text{ sec},$$
$$E_t - E_i = 4.6kT \text{ or } 1.3\ kT,$$

where we have used the following constants:[14]

$$n_i = 10^{-10} \text{ cm}^{-3},$$
$$D_p = 11.1 \text{ cm}^2/\text{sec},$$
$$D_n = 2.77 D_p,$$
$$E_g = 1.21ev \text{ at } 0° \text{ K}.$$

The value of $E_t - E_i$ cannot be uniquely determined from this experiment since the results only give cosh $[(E_t - E_i)/kT + (1/2) \ln(\tau_{p0}/\tau_{n0})]$ which makes the sign uncertain. However, the value of $E_t - E_i$ obtained is in good agreement with the result of Pell and Roe.[5]

The theoretical calculations and the experimental measurements are presented in Figs. 11 and 12. Good agreement is obtained over the entire range of more than 9 decades of junction current. In addition to the three-point-match, we have also taken into consideration the contact resistance drop which accounts for

[14] Morin and Maita, "Electrical properties of silicon containing arsenic and boron," *Phys. Rev.*, vol. 96, pp. 28–35; October 1, 1954. M. B. Prince, "Drift mobility in semiconductors. II. Silicon," *Phys. Rev.*, vol. 93, pp. 1204–1206; March 15, 1954.

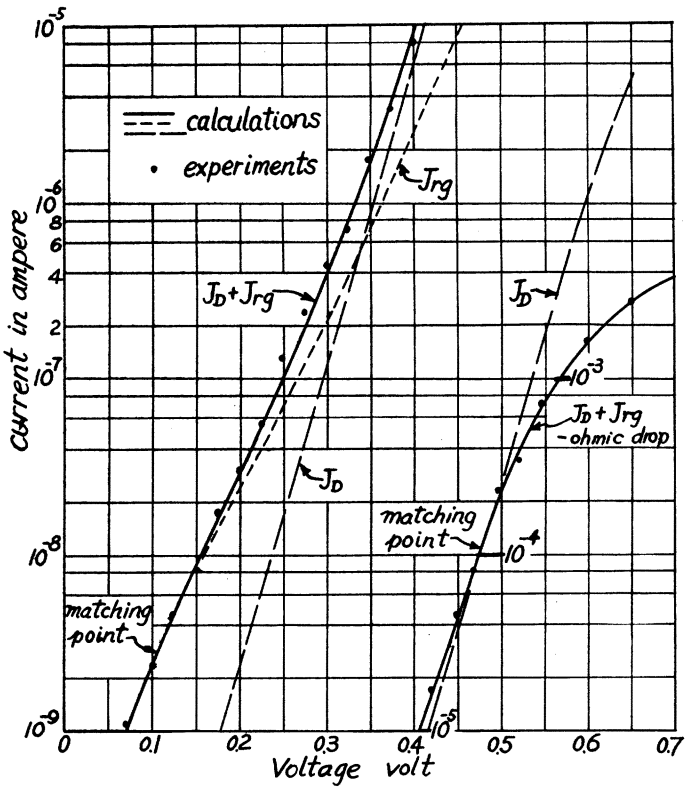


Fig. 11—Forward characteristics of a silicon $p$-$n$ junction.

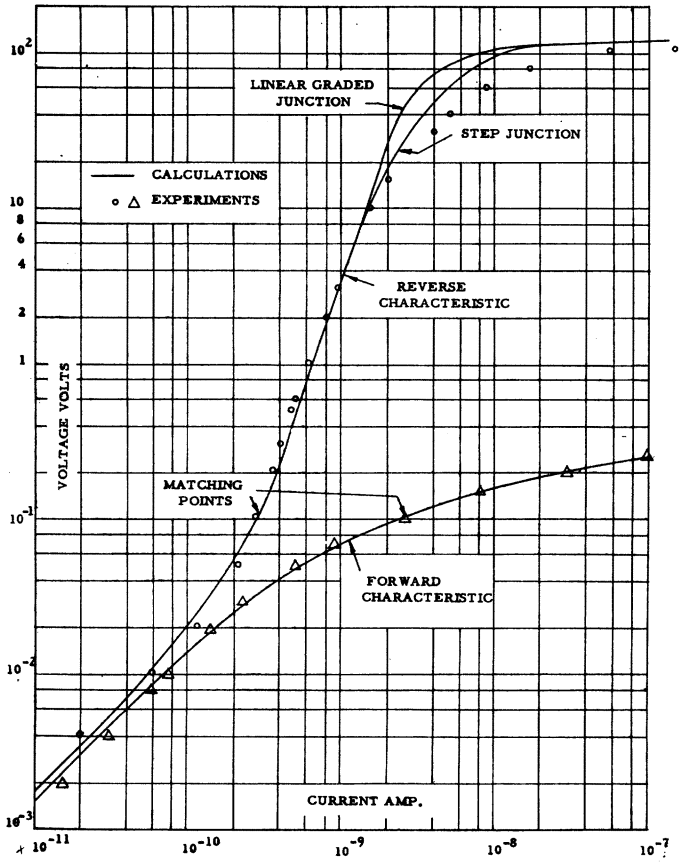


Fig. 12—Silicon $p$-$n$ junction characteristics.

the slow increase of the large forward current. The avalanche multiplication near the avalanche breakdown voltage is also considered. In this region, the experimental measured currents were found for all cases to be always greater than the calculated values. This may be due to the dependence of the lifetimes on the electric field and due to surface breakdown.

Additional data are shown in Figs. 13(a) and (b), on the next page, for silicon diodes of different base resistivities and surface concentrations. Table II shows the calculated lifetimes and trap energy levels from the experimental data. The energy level of the recombination-generation center or trap is at about $+4kT$ from the intrinsic Fermi level. This is in fair agreement with the temperature data shown in Fig. 14.

TABLE II

| Unit No. | 352-10 | 354-3 | 354-4 | 315A2 | 317A18 |
|---|---|---|---|---|---|
| Type | $P^+N$ | $P^+N$ | $P^+N$ | $N^+P$ | $N^+P$ |
| $\rho$(Ω-cm) | 2.4 | 2.4 | 2.4 | 21 | 21 |
| $C_0$ surface cm$^{-3}$ | $5\times10^{21}$ | $5\times10^{21}$ | $5\times10^{21}$ | $10^{22}$ | $3\times10^{18}$ |
| $\tau_{p0}$ ($\mu$sec) | 0.035 | 0.035 | 0.039 | 0.05 | 0.15 |
| $\tau_{n0}$ ($\mu$sec) | 0.65 | 0.69 | 0.69 | 0.07 | 0.012 |
| cosh $\epsilon_t$ | 6.3 | 5.3 | 6.0 | 2.2 | 5.5 |
| $((E_t-E_i)/kT)_+$ | 4.0 | 3.9 | 3.9 | 1.3 | 3.7 |
| $((E_t-E_i)/kT)_-$ | −1.1 | −0.9 | −1.0 | −1.6 | −1.2 |

Under certain conditions, the surface leakage current may be important in silicon $p$-$n$ junctions.[15,16] If the surface charge is smaller than the fixed charge of the impurities, it can be shown that the surface current, produced by recombination-generation centers or surface states at the circumferential surface of the junction, will follow the same voltage dependence, namely, $V^{1/2}$ or $V^{1/3}$, under the large reverse bias condition.

In order to separate the recombination-generation current due to surface centers from that due to volume centers we have made experimental measurements on $p$-$n$ junctions with extremely large and small ratios of junction area to circumference. The geometries are shown in Fig. 15. The results indicate that the surface current is negligible compared with bulk current for freshly etched junctions.

## VII. Conclusion

In this paper we have used a model of the single level uniformly distributed Shockley-Read recombination-generation centers to explain the $p$-$n$ junction characteristics. This model explains both the nonsaturable reverse characteristics and the apparent exp $(qV/nkT)$ dependence of the forward current of typical silicon

[15] M. Culter and H. M. Bath, "Surface leakage current in silicon fused junction diodes," Proc. IRE, vol. 45, pp. 39–43; January, 1957.

[16] W. T. Eriksen, H. Statz, and G. A. DeMars, "Excess surface currents on germanium and silicon diodes," *J. Appl. Phys.*, vol. 28, pp. 133–139; January, 1957.

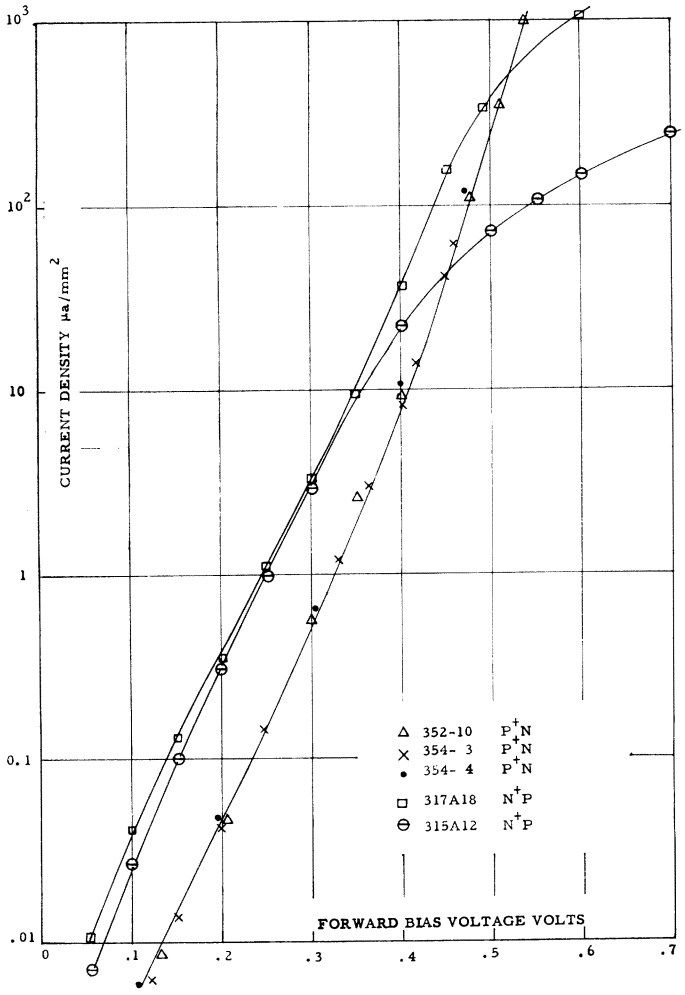


(a)

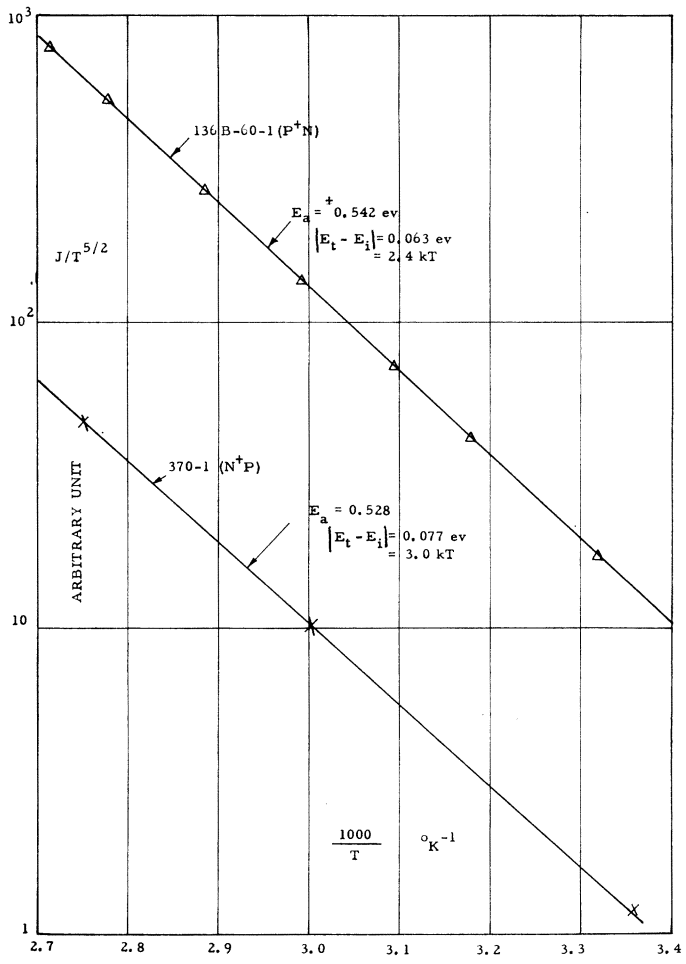


Fig. 14—Activation energy of recombination-generation centers in silicon *p-n* junctions.

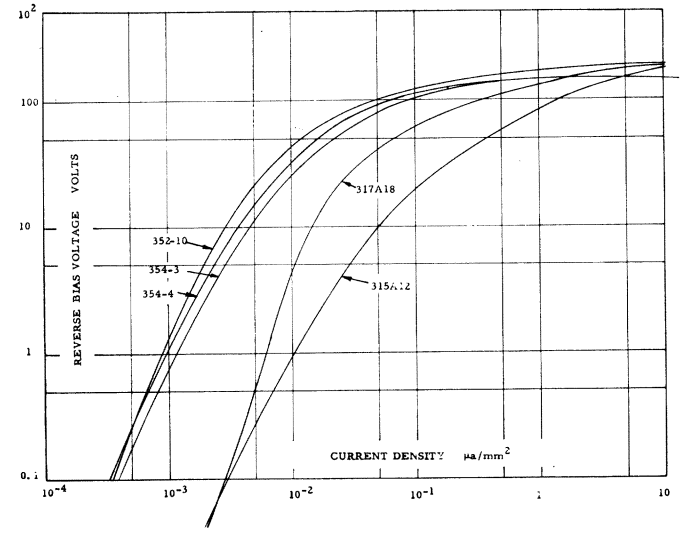


(b)

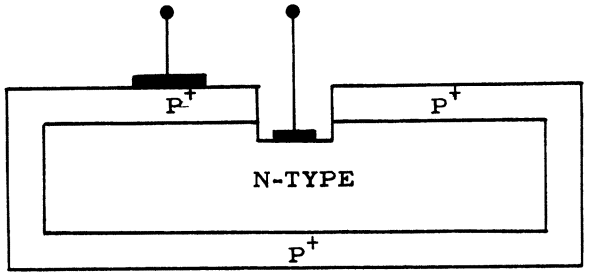


(a)

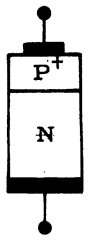


(b)

Fig. 13—(a) Experimental forward characteristics of silicon *p-n* junctions. (b) Experimental reverse characteristics of silicon *p-n* junctions.

Fig. 15—Geometry for separating surface and bulk currents; (a) large junction area to circumference ratio geometry; (b) small junction area to circumference ratio geometry.

$p$-$n$ junctions. The recombination of the carriers in the space charge layer also explains the variation of the current amplification factor of a silicon transistor at low emitter current density.

## Appendix I

### Variation of the Quasi-Fermi Levels in the Space Charge Layer

The hole current can be written as

$$J_p = -q\mu_p p(d\phi_p/dx). \tag{32}$$

Substituting the expression for $p$ from (19) into (32) the following differential equation can be obtained.

$$\frac{d}{ax}\exp\frac{q}{kT}(\phi_p-\Psi)-\frac{q}{kT}\left(\frac{d\Psi}{dx}\right)\exp\frac{q}{kT}(\phi_p-\psi) = -\frac{J_p}{q\mu_p n_i}. \tag{33}$$

The solution of this equation is

$$\exp(q\phi_p/kT) = C-\int\exp\left(\frac{q}{kT}\Psi\right)\frac{J_p dx}{q\mu_p n_i}. \tag{34}$$

To calculate the variation of the quasi-Fermi potential variation across the space charge layer we use the linear approximation for the hole current density $J_p$, and for the electrostatic potential variation. Thus, for $-\frac{1}{2}W<x<\frac{1}{2}W$

$$J_p = J(1-2x/W) \tag{35}$$

and

$$\Psi = (\Psi_D-\delta\phi)x/W, \tag{36}$$

where $\Psi_D$ is the built-in voltage, $\delta\phi$ is the applied voltage and $W$ is the space charge layer width. By the evaluation of the integral of (34) with these approximations, the following relation is obtained for the quasi-Fermi potentials for holes at the edges of the space charge layer.

$$\exp\frac{q}{kT}\left[\phi_p\left(\frac{W}{2}\right)+\phi_p\left(\frac{-W}{2}\right)\right]\cdot\sinh\frac{q}{2kT}\left[\phi_p\left(\frac{W}{2}\right)-\phi_p\left(\frac{-W}{2}\right)\right] = (JW/q\mu_p n_i)\left[\frac{\sinh(\theta_1/2)}{\theta_1}-\exp(-\theta_1/2)\right]\Big/\theta_1 \tag{37}$$

where $\theta_1=(\Psi_D-\delta\phi)q/kT$.

For forward bias, $\theta_1$ is small and (37) reduces to

$$\exp\left[\phi_p\left(\frac{W}{2}\right)+\phi_p\left(\frac{-W}{2}\right)\right]\frac{q}{2kT}\cdot\sinh\left[\phi_p\left(\frac{W}{2}\right)-\phi_p\left(\frac{-W}{2}\right)\right]\frac{q}{2kT} = JW/2q\mu_p n_i. \tag{38}$$

Thus, for a forward current of $J=2$ amp/cm$^2$, $W=10^{-6}$ cm and $\mu_p=500$ for Si, the maximum drop of the quasi-Fermi potential for holes is

$$\sinh q\delta\phi_p/2kT = 0.4\exp-\left[\phi_p\left(\frac{W}{2}\right)\frac{q}{2kT}\right].$$

The exponential factor on the right-hand side cannot be more than 1. This is easily seen from Fig. 5 if the reference potential is at $(\frac{1}{2})[\phi_p(x)+\phi_n(x)]_{x=0}$ as was implied in (36). In addition, a current less than $J$ should be used as shown in Fig. 5. Thus the upper limit of the drop of the quasi-Fermi level in the space charge layer is about $(kT/q)$ and is indeed very small.

For the large reverse-bias case, $\theta_1>5$, the situation is quite different. Eq. (37) can be approximated by

$$\sinh\left[\phi_p\left(\frac{W}{2}\right)-\phi_p\left(\frac{-W}{2}\right)\right]\frac{q}{2kT} = \exp\left\{-\left[\phi_p\left(\frac{W}{2}\right)+\phi_p\left(\frac{-W}{2}\right)\right]\frac{q}{2kT}\right\}\cdot\left(\frac{JW}{q\mu_p n_i}\right)\frac{e^{1/2\theta_1}}{\theta_1^2}. \tag{39}$$

Thus, for $J=10^{-6}$ amp/cm$^2$, $W=10^{-4}$ cm and $\theta_1=100$, the drop of the quasi-Fermi potential is

$$\sinh(q\delta\phi_p/2kT) = \exp\left[80.7-\phi_p\left(\frac{W}{2}\right)q/2kT\right].$$

By successive approximation it can be shown that the drop of the quasi-Fermi potential for holes is approximately equal to the applied voltage as indicated in Fig. 4.

For small bias, $\theta_1$ is equal to the built-in voltage. For $\theta_1=20$, $J=10^{-8}$ amp/cm$^2$, and $W=10^{-5}$ cm the drop of the quasi-Fermi potential for holes is approximately

$$\sinh\delta\phi_p q/2kT = \exp(-12.5-\delta\phi q/kT).$$

Thus the drop is appreciable only when the reverse-bias is greater than about $12.5kT/q$.

## Appendix II

### Avalanche Multiplication of the Generated Carriers in the Space Charge Layer

Suppose that the $p$-$n$ junction shown in Fig. 16 is biased in the reverse direction. Hole current density per unit area $J_p(x)$ flows toward the left, and electron current density per unit area $J_n(x)$ flows toward the right. There is also a net steady-state generation of the hole-electron pairs in the space charge region of $U$ per unit volume per unit time from the Shockley-Read-Hall generation-

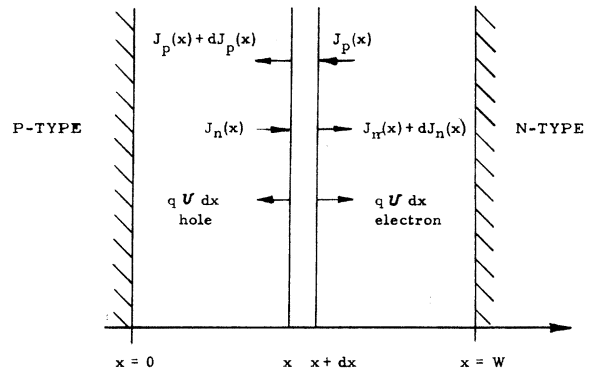


Fig. 16—Avalanche multiplication of electron and hole currents in the space charge layer of a reverse biased $p$-$n$ junction.

recombination centers. We define, as done by McKay and Miller[17] the ionization coefficients as follows:

$\alpha$ = no. of electron-hole pairs produced per cm travel of an electron.

$\beta$ = no. of electron-hole pairs produced per cm travel of a hole.

We assume that $\alpha$ and $\beta$ are functions of the local electric field only and neglect the past history of the carriers. We also neglect the space charge effect or the interaction between the carriers. The change of electron current in $dx$ per unit area is

$$dJ_n(x) = \alpha J_n(x)dx + \beta J_p(x)dx + qUdx, \tag{40}$$

where the first term on the right comes from the multiplication of the electron current going into $dx$ from the side $x$, and the second term comes from the electrons produced by holes going into $dx$ from the side $x+dx$. Similarly, the change of the hole current in $dx$ per unit area is

$$-dJ_p(x) = \alpha J_n(x)dx + \beta J_p(x)dx + qUdx, \tag{41}$$

and the sum of the two incremental currents satisfies the condition that the total current is space constant, namely

$$J = J_p(x) + J_n(x) = \text{independent of position.} \tag{42}$$

To solve the two simultaneous differential equations we use the following boundary conditions. At $x=0$, $J_n=J_{n0}$ and at $x=W$, $J_p=J_{p0}$. Substituting (42) into (40) and (41) the electron and the hole current satisfies the following equations:

$$dJ_n(x)/dx = (\alpha - \beta)J_n(x) + \beta J + qU \tag{43}$$

and

$$dJ_p(x)/dx = (\alpha - \beta)J_p(x) - \alpha J - qU. \tag{44}$$

[17] K. G. McKay, "Avalanche breakdown in silicon," *Phys. Rev.*, vol. 94, pp. 877–884; May 15, 1954.
S. L. Miller, "Ionization rates for holes and electrons in silicon," *Phys. Rev.*, vol. 105, pp. 1246–1249; February 15, 1957.

The solutions are

$$J_n(x) = e^{-\int^x(\alpha-\beta)dx} \cdot \int_0^x (\beta J + qU)e^{\int^x(\alpha-\beta)dx}dx + J_{n0} \tag{45}$$

and

$$J_p(x) = e^{-\int^x(\alpha-\beta)dx}\int_W^x (\alpha J + qU)e^{\int^x(\alpha-\beta)dx}dx + J_{p0}. \tag{46}$$

Thus, the total current is

$$J = J_p(x) + J_n(x) = \frac{J_{p0} + J_{n0} + e^{-\int^x(\alpha-\beta)dx}\int_0^W qUe^{\int^x(\alpha-\beta)dx}dx}{1 - \int_0^x \beta e^{\int^x(\alpha-\beta)dx}dx - \int_x^W \alpha e^{\int^x(\alpha-\beta)dx}dx}. \tag{47}$$

For $\alpha=\beta$, $J$ reduces to

$$J = \frac{J_{p0} + J_{n0} + \int_0^W qUdx}{1 - \int_0^W \alpha dx} = M(J_{p0} + J_{n0} + \int_0^W qUdx), \tag{48}$$

where $M$ is the current multiplication factor given by

$$M = \left(1 - \int_0^W \alpha dx\right)^{-1}.$$

Eq. (48) indicates that for $\alpha=\beta$ the generated current in the space charge layer, $\int qUdx$, acts as if it is injected into the layer as far as avalanche multiplication is concerned.

## Appendix III

### Activation Energy of the Traps

The thermal activation energy of the traps is obtained from the slope of a plot of the log of the reverse current as a function of the reciprocal of temperature at a constant reverse-bias.

Consider the range of $-\theta>5$ where $\theta$ is the normalized applied bias $(\phi_p-\phi_n)q/kT$. The function $f(b)$ for this case can be approximated by $(\log 2b)/b$ and the recombination-generation current can be written as

$$\log [J_{rg}/J_0(kT)^{5/2}] = \log\left[\frac{n_i}{\theta(kT)^{5/2}\cosh\left(\frac{E_t - E_i}{kT} + \frac{1}{2}\ln\frac{\tau_{p0}}{\tau_{n0}}\right)}\right]. \tag{49}$$

Since $n_i$ is proportional to $T^{3/2}\exp(-E_{g0}/2kT)$ and $b>10$ for the restriction imposed on the reverse-bias, the activation energy can be obtained by differentiating (49) and is

$$E_a = -\frac{1}{2}E_{g0} - (E_t - E_i) \cdot \tanh\left(\frac{E_t - E_i}{kT} + \ln\sqrt{\frac{\tau_{p0}}{\tau_{n0}}}\right), \quad (50)$$

where $E_{g0}$ is the energy gap width at zero temperature. Thus for deep traps, $E_t \doteq E_i$ and the trap energy cannot be obtained exactly unless measurements are done at low temperatures. For shallow traps, accurate energy level can be obtained in the room temperature range.

If

$$\left(\frac{E_t - E_i}{kT} + \ln\sqrt{\frac{\tau_{p0}}{\tau_{n0}}}\right)$$

is greater than about 2, the last term of (50) reduces to the absolute value of $E_t - E_i$. The energy of the traps can be obtained from

$$\pm(E_t - E_i) = E_a + E_{g0}/2. \quad (51)$$

## Appendix IV

### Currents Outside Space Charge Layer

In this appendix we shall obtain the diffusion current flowing in the $n$ region of a forward biased $P^+N$ junction. The approach here is slightly different from that given in the text but is similar to that generally used in the literature.[18] We take into consideration both the nonlinear recombination rate and the high-level boundary condition.

The assumptions of this analysis are:

1) The space charge due to the divergence of the electric field $E$ is small compared with the fixed charge $N$ due to the impurities. This assumption implies that $n = p + N$.

2) The imrefs are approximately constant in the transition region and their difference is only slightly less than the applied voltage.

The second assumption above is a very good one at not very large current densities. At very high current densities the ohmic resistance drop in the $N$ region becomes important. This ohmic drop can be calculated from the total drop of the electron imref in this region, namely, $J = qD_nN \text{ grad } \phi_n$, where $J$ is the total current density. This correction of the voltage at the junction can then be made.

The boundary condition follows from the second assumption and may be written as

$$pn = n_i^2 \exp(\phi_p - \phi_n)q/kT = n_i^2 \exp(qV/kT), \quad (52)$$

where $V$ is $V$ (applied) $-\delta\phi_n$ and $\delta\phi_n$ is the electron imref drop in the $N$ region.

We shall start from the following relations:

$$\begin{aligned} K\epsilon_0 \text{ div } E &= q(p - n + N)^{++},^{19} \\ J_p &= qD_p(qEp/kT - \text{grad } p), \\ J_n &= qD_n(qEn/kT + \text{grad } n), \\ \text{div } J_p &= -qU, \\ \text{div } J_n &= qU, \end{aligned} \quad (53)$$

where the notations are defined before.

For the one-dimension case with uniform doping in the $n$ region the above equations can be reduced to

$$d^2p/dx^2 = (D_n + D_p)U/2D_pD_n \quad (54)$$

and

$$qE/kT = \frac{J - qD_p(b-1)dp/dx}{qD_p[p(1+b) + bN]}, \quad (55)$$

where $b = D_n/D_p$ differs from the same symbol used previously in the text. The recombination-generation rate from (6) becomes

$$U = (\tau_{p0} + \tau_{n0})^{-1} \cdot \left[p + N - p_0 - \frac{p_0(N - p_0) + n_i^2}{p + p_0}\right] \quad (56)$$

where

$$p_0 = \frac{\tau_{p0}n_1 + \tau_{n0}p_1 + \tau_{p0}N}{\tau_{p0} + \tau_{n0}}. \quad (57)$$

We shall use the following boundary conditions derived from our assumptions.

At $x = 0$, the edge of the space charge layer on the $n$-region side

$$p(0)n(0) = n_i^2 \exp(qV/kT)$$

and

$$n(0) = p(0) + N$$

so that

$$p(0) = [\sqrt{1 + (4n_i^2/N^2)\exp(qV/kT)} - 1]N/2. \quad (58)$$

At $x = \infty$, $p(\infty) = p_n$ and let grad $p = 0$, then

$$\frac{qE(\infty)}{kT} = \frac{J}{qD_n[N + p_n(1+b)/b]} \quad (59)$$

[18] E. S. Rittner, "Extension of the theory of the junction transistor," *Phys. Rev.*, vol. 94, pp. 1161-1171; June 1, 1954.
T. Misawa, "A note on the extended theory of the junction transistor," *J. Phys. Soc. Japan*, vol. 11, pp. 728-739; July, 1956.
W. T. Read, Jr., "Theory of the swept intrinsic structure," *Bell Sys. Tech. J.*, vol. 35, pp. 1239-1284; November, 1956.
D. A. Kleinman, "The forward characteristic of the PIN diode," *Bell Sys. Tech. J.*, vol. 35, pp. 685-706; May, 1956.
K. B. Tolpygo, "Emission capability of an abrupt $p$-$n$ transition and its effect upon the conductivity of a semiconductor," *J. Tech. Physics*, vol. 1, pp. 287-305 (English translation, Am. Inst. of Phys.)
J. A. Swanson, "Diode theory in the light of hole injection," *J. Appl. Phys.*, vol. 25, pp. 314-323; March, 1954.

[19] Contribution from the traps is neglected.

and

$$J_p(\infty) = \frac{Jp_n}{(1+b)p_n + bN}. \tag{60}$$

The gradient of the hole density can now be solved. Eqs. (54) and (56) give

$$d^2p/dx^2 = (2L_0^2)^{-1} \cdot \left[p + N - p_0 - \frac{p_0(N-p_0)+n_i^2}{p+p_0}\right], \tag{61}$$

where

$$L_0^{-2} = (D_n^{-1} + D_p^{-1})(\tau_{p0} + \tau_{n0}). \tag{62}$$

Eq. (61) can be easily integrated to give

$$(dp/dx)^2 = L_0^{-2}[p^2/2 - p_n^2/2 + (N-p_0)(p-p_n) - (p_0(N-p_0)+n_i^2)\ln(p+p_0)/(p_n+p_0)]. \tag{63}$$

We are interested in the solution at $x=0$ since at this point the relation between the total current and the hole current can be written as

$$J = J_p(0) + J_{rg}, \tag{64}$$

if the electron current in the $p$ region is neglected. Using these results we can deduce the following relations for the total current and the hole current at $x=0$.

$$J = \frac{J_{rg}[(1+b)p(0)+bN] - qD_n[2p(0)+N]dp(0)/dx}{b[p(0)+N]} \tag{65}$$

and

$$J_p(0) = \frac{J_{rg}p(0) - qbD_p[2p(0)+N]dp(0)/dx}{b[p(0)+N]}. \tag{66}$$

Thus, (58), (65), and (66) represent the complete solution.

The asymptotic forms of the above results will be considered. The regions to be considered are the low-level case $p(0) \leqq N/10$, the medium-level case $p(0) \geqq N$, and the high-level case $p(0) \geqq 10N$.

*1) Low-Level Case, $p(0) \leqq N/10$*

For this case the total current is given by

$$J = J_{rg} + qp_nL_{p0}\sqrt{(1+b^{-1})/2}[\exp(qV/kT) - 1]/\tau_{p0}$$

and

$$J_p(0) = qp_nL_{p0}\sqrt{(1+b^{-1})/2}[\exp(qV/kT) - 1]/\tau_{p0}$$

where $L_{p0} = \sqrt{D_p\tau_{p0}}$. The hole current varies exponentially with distance. However, the expression for the hole current at $x=0$ given above differs from the ordinary low-level relation by a factor $\sqrt{(1+b^{-1})/2}$. This comes from the difference of the assumption made. In the ordinary low-level theory it is assumed that not only the charge neutrality holds but the electric field is also zero everywhere outside the junction. The present assumption of negligible charge due to the divergence of electric field is less restrictive than the usual one.

For a one ohm-cm material with 1-microsecond lifetime the maximum range of validity of the above quantities are listed below for germanium and silicon at room temperature.

| | $J_p(0)_{max}$ amp/cm² | $V_{max}$ volts |
|---|---|---|
| Ge | 0.16 | 0.15 |
| Si | 0.25 | 0.57 |

*2) Medium-Level Case $p(0) \geqq N$*

For this case the current densities cannot be reduced to simple expressions. However, the hole gradient at $x=0$ can be written as

$$\text{grad } p(0) = -[p^2(0) + 2(N-p_0)p(0)]/\sqrt{2}\,L_0.$$

The electric fields can be obtained approximately as

$$qE(\infty)/kT = 3/(2bL_0)$$

and

$$qE(0)/kT = 1/(2L_0),$$

thus the electric field is relatively constant over the entire $n$ region.

For a one ohm-cm material with 1-microsecond lifetime, the following list summarizes the minimum current density and minimum applied voltage for this range at room temperature.

| | $J_{min}$ amp/cm² | $V_{min}$ volts |
|---|---|---|
| Ge | 2.9 | 0.18 |
| Si | 4.6 | 0.6 |

*3) High-Level Case $p(0) \geqq 10N$*

For this case the boundary condition becomes

$$p(0) = n_i \exp(qV/2kT)$$

and the current densities are

$$J = J_{rg}(1+b)/b + \sqrt{2}qD_pp(0)/L_0$$

and

$$J_p(0) = J_{rg}/b + \sqrt{2}qD_pp(0)/L_0.$$

It has been shown in the text that for this case the recombination current in the space charge layer is negligible compared with the diffusion current. Thus the total current is essentially equal to the hole current at $x=0$, and varies as $\exp(qV/2kT)$. This region is at a much higher current density than the similar region considered for the recombination-generation current in the space charge layer.

We need to examine the electric field and its divergence at the boundaries to verify the validity of our assumptions. At the lowest applied voltage for this case of large bias the electric fields can be obtained by using (58) and (59).

$$qE(0)/kT = (1/\sqrt{2}L_0)$$

$$qE(\infty)/kT = (1/\sqrt{2}L_0)\ 2p(0)/bN.$$

Thus the electric field varies about a factor of 10 at least. The gradient of the electric field can be obtained by differentiating (55). At $x=\infty$, $dE/dx$ is zero and at $x=0$ the electric field is about

$$(q/kT)(dE/dx) = 1/2L_0^2$$

at the lowest injection limit. This corresponds to about 25 v/cm for a 1-microsecond lifetime material at room temperature. The quantity $(K\epsilon_0/q)dEdx$ can now be compared with $p-n+N$ from (53). Using the values given above we obtain

$$p - n + N \gg 7.6 \times 10^{10}\ \text{cm}^{-3},$$

which is usually satisfied since $N$ is of the order of $10^{15}$ $\text{cm}^{-3}$ for silicon of a few ohm-cm resistivity.

We shall give again a list indicating the limiting values of current density and voltage for this range.

| | $J_{min}$ amp/cm² | $V_{min}$ volt |
|---|---|---|
| Ge | 27 | 0.34 |
| Si | 43 | 0.75 |

ACKNOWLEDGMENT

The authors wish to acknowledge the helpful discussions with their colleagues at the Shockley Semiconductor Laboratory. The diffused silicon materials were prepared by D. Grunwald, and some of the data were taken by Dr. S. M. Fok and M. Asemissen.

(*Note added in proof:* The forward characteristics of germanium *p-n* junctions at low temperatures have recently been investigated independently by M. Bernard using the same model. "Mesures in fonction de la temperature du Courant," *J. Electronics*, vol. 2, pp. 579–596; May, 1957.)

# Digital Compensation for Control and Simulation*

JULIUS TOU†, SENIOR MEMBER, IRE

*Summary*—**This paper describes a technique for improving the performance of digital feedback control systems and operational digital simulators by making use of the computer to perform information programming or data processing. The system stability can be improved and the system error can be reduced by digital programming of the input and error signals together with digital correction computations. This technique of digital compensation is illustrated by an example.**

## INTRODUCTION

AMONG the many performance criteria for feedback control systems, the stability and accuracy considerations are of primary importance. Considerable amount of work has been done for improving the performance of feedback control systems and a number of methods have been published in the literature. With the rapid advance of computer design techniques and their applications, there arose a new type of system for control and simulation which involves a digital computer. Such systems are often called digital control systems and operational digital simulators.

A typical digital control system or a channel of an operational digital simulator is shown in Fig. 1, which

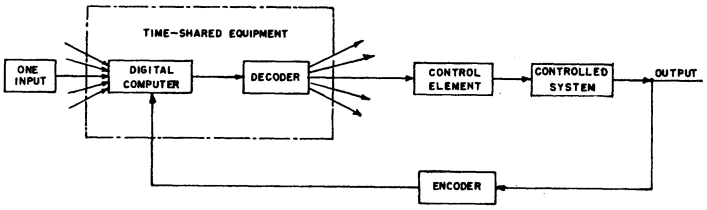


Fig. 1—A typical digital control system or a channel of an opertional digital simulator.

consists of a digital computer, a decoder, an encoder and the control element and controlled system. The computer performs error detection and system compensation. The decoder converts signals in digital or sampled form into continuous form. The encoder converts continuous data into sampled form or digital code. The stability and accuracy of such control systems can be improved by designing a suitable program for the computer. The technique of digital programming compensation will be described in this paper.

One of the most powerful tools for analyzing and designing digital and sampled-data feedback control systems and simulators is the $Z$-transform method.[1,2] Since this method of approach will be employed in this

* Original manuscript received by the IRE, August 13, 1956; revised manuscript received, June 11, 1957. This article is based upon the paper "High Accuracy Operational Digital Simulation" presented by the author at the first Natl. Simulation Conf., in Dallas, Tex., January, 1956.

† Purdue Univ., Lafayette, Ind. Formerly with Moore School of Elec. Eng., Univ. of Pennsylvania and the Philco Corp., Philadelphia, Pa.

[1] R. H. Barker, "The pulse transfer function and its application to sampling servo systems," *Proc. IEE*, vol. 99, pt. IV, pp. 302–317; December, 1952.

[2] J. R. Ragazzini and L. A. Zadeh, "The analysis of sampled-data systems," *AIEE Trans.*, vol. 71, pp. 225–232; November, 1952.